A Climatology of Cell Mergers with Supercells and Their Association with Mesocyclone Evolution

MATTHEW D. FLOURNOY,[a,b] ANTHONY W. LYZA,[a,b] MARTIN A. SATRIO,[c] MADELINE R. DIEDRICHSEN,[c] MICHAEL C. CONIGLIO,[b,c] AND SEAN WAUGH[b]

[a] *Cooperative Institute for Severe and High-Impact Weather Research and Operations, University of Oklahoma, Norman, Oklahoma*
[b] *NOAA/National Severe Storms Laboratory, Norman, Oklahoma*
[c] *School of Meteorology, University of Oklahoma, Norman, Oklahoma*

(Manuscript received 29 July 2021, in final form 7 December 2021)

ABSTRACT: In this study, we present a climatology of observed cell mergers along the paths of 342 discrete, right-moving supercells and their association with temporal changes in low-level mesocyclone strength (measured using azimuthal shear). Nearly one-half of the examined supercells experience at least one cell merger. The frequency of cell merger occurrence varies somewhat by geographical region and the time of day. No general relationship exists between cell merger occurrence and temporal changes in low-level azimuthal shear; this corroborates prior studies in showing that the outcome of a merger is probably sensitive to storm-scale and environmental details not captured in this study. Interestingly, we find a significant inverse relationship between premerger azimuthal shear and the subsequent temporal evolution of azimuthal shear. In other words, stronger low-level mesocyclones are more likely to weaken after cell mergers and weaker low-level mesocyclones are more likely to strengthen. We also show that shorter-duration cell merger "events" (comprising multiple individual mergers) are more likely to be associated with a steady or weakening low-level mesocyclone whereas longer-duration cell merger events (3–4 individual mergers) are more likely to be associated with a strengthening low-level mesocyclone. These findings suggest what physical processes may influence the outcome of a merger in different scenarios and that the impact of these processes on low-level mesocyclone strength may change depending on storm maturity. We establish a baseline understanding of the supercell–cell merger climatology and highlight areas for future research in how to better anticipate the outcomes of cell mergers.

SIGNIFICANCE STATEMENT: A common assumption in idealized supercell simulations is that the background environment is homogeneous. Cells merging into a primary supercell represent one of many ways in which the environment might be significantly inhomogeneous. This study analyzes the paths of 342 supercells with a particular focus on how cell merger occurrence influences the strength of the low-level mesocyclone. Almost one-half of all supercells experience at least one cell merger. Supercells are more likely to weaken after a cell merger event if the premerger mesocyclone was strong or if the merger event is relatively short, and vice versa for the likelihood for a supercell to strengthen. These findings are important for those interested in short-term predictions of supercell evolution in response to cell mergers and suggest what dynamic processes may play a role in governing these relationships.

KEYWORDS: Convective-scale processes; Supercells; Radars/radar observations; Short-range prediction

1. Introduction and motivation

A common assumption in idealized simulations of supercells is that the base-state environment is homogeneous. The occurrence of a secondary cell merging with the primary supercell (henceforth referred to as a cell merger) is one of several ways in which the inflow of a supercell might be significantly inhomogeneous. Observational studies detailing cell mergers with finescale spatiotemporal resolution are scarce. Notable exceptions are Wurman et al. (2007), which provides an analysis of Doppler-on-Wheels radar observations of the 26 May 1997 Kiefer, Oklahoma, tornadic supercell that featured two separate cell merger events, and Klees et al. (2016), which analyzed the environments of both a nontornadic and a tornadic supercell on 10 June 2010 with a suite of instruments including mobile radars, mesonets, and rawinsondes. Wurman et al. (2007) found that each of the two cell mergers in their case coincided with quick tornadic development and subsequent dissipation within a time frame of 10 min. Klees et al. (2016) determined that one cell merger weakened the nontornadic supercell and eventually led to dissipation while the other cell merger may have strengthened the midlevel mesocyclone of the tornadic supercell prior to tornadogenesis. These two studies demonstrate 1) the complexity of cell merger impacts on storm morphology depending on the cell merger intensity, size, and placement within the supercell inflow environment and 2) that a larger study would be beneficial to identify possible trends.

In addition to singular supercell event studies, several larger storm event studies have been conducted relating cell mergers to supercell reflectivity and rotational trends as well as tornadogenesis. Lee et al. (2006) analyzed 26 cell merger events associated with the 19 April 1996 Illinois tornado outbreak. Each merger event was binned into one of five

Corresponding author: Matthew Flournoy, matthew.flournoy@noaa.gov

DOI: 10.1175/MWR-D-21-0204.1

© 2022 American Meteorological Society. For information regarding reuse of this content and general copyright information, consult the AMS Copyright Policy (www.ametsoc.org/PUBSReuseLicenses).

Brought to you by NOAA Central Library | Unauthenticated | Downloaded 03/14/22 08:34 PM UTC

categories dependent on reflectivity tendencies as the merging cell collided with the supercell and then was compared with the reflectivity of the resultant storm and tornado production. Similar to Klees et al. (2016), around one-half of the merger events from Lee et al. (2006) resulted in a strengthening of the supercell's azimuthal shear. Additionally, 54% of tornadogenesis events in the 1996 case corresponded with a cell merger event within a defined 15-min window on either side of the tornado report. Rogers and Weiss (2008) built a dataset of 91 tornado reports across the Texas Panhandle and southern Great Plains between 1999 and 2006 that included multiple storm mode types (discrete, cluster, broken line, and line). Similar to Lee et al. (2006), they found that about 54% of the tornado reports were associated with a merger event during the 15-min window. Rogers (2012) created a larger dataset containing 669 tornado reports (EF2+ on the enhanced Fujita scale) from 2006 to 2010 to determine the effect of cell merger events in the environments of significant tornadoes. Unlike Lee et al. (2006) and Rogers and Weiss (2008), Rogers (2012) found that only 27% of the tornado reports corresponded to a cell merger event during the 15-min window. The disparity between the studies could be due to the differences in the datasets analyzed (i.e., the Lee et al. dataset was much smaller), or the possibility that significant tornadoes are less likely to occur in association with a cell merger than weaker tornadoes.

Numerical models have also been used to simulate nascent convective clouds and ordinary cells, showing that intensification often occurs after merging events (e.g., Simpson et al. 1980; Tao and Simpson 1989; Westcott 1994; Kogan and Shapiro 1996; Pozo et al. 2006). However, because of the amplified pressure perturbation fields in the vicinity of supercells relative to ordinary cells (Davies-Jones 2002), cell merger interactions with supercells could be expected to be much more complex. Bluestein and Weisman (2000) modeled storms forming in an environment conducive for collisions between weaker left-moving supercells and more dominant right-moving supercells; indeed, complexities were found with one cell interaction event leading to a brief increase in low-level vorticity but all other interactions having destructive tendencies. Similarly, Jewett et al. (2006) showed the realization of destructive or constructive mergers to be highly dependent on the location and orientation of the merging cell relative to the right-moving supercell.

More recently, Hastings and Richardson (2016) simulated collisions between right-moving dominant supercells and ordinary cells forming in the same environment using Cloud Model 1 (CM1; Bryan et al. 2003). The simplest situation arose when outflow from the merging cell cuts off inflow to the supercell, resulting in a destructive merger. However, if the outflow is not cold or deep enough, the resultant interaction is dependent on the minimum distance between the updraft maxima. Namely, it is found that if the minimum separation is 1) less than 10 km, the two updrafts collide and merge into a classic supercell; 2) greater than 20 km, the new cell merges into the forward-flank region and a dual-cell system develops; and 3) between 10 and 20 km, the updrafts converge via an updraft bridge and cold pool surge resulting in either bow echo formation or a high-precipitation supercell. In contrast to Bluestein and Weisman (2000), nearly all merger events were accompanied by a stronger resultant supercell than the control simulation. However, Hastings and Richardson (2016) recognize that the chosen shear profile may play a large role in merger interactions, as modifying the hodograph to be favorable for splitting supercells led to results more in agreement with Bluestein and Weisman (2000).

In situations where merger events play a constructive role, numerical studies have shown that cell mergers favorably modify the vorticity budget of the midlevel mesocyclone. For example, through circulation analysis, Hastings et al. (2014) hypothesized that rear-flank mergers increase vorticity through baroclinic generation. Likewise, Tanamachi et al. (2015) analyzed the 24 May 2011 El Reno, Oklahoma, tornado in the period between two consecutive tornadoes (EF3 and EF5) when the supercell merged with a weaker cell. It was concluded that while the merger itself was not entirely responsible for tornado occlusion and subsequent reformation, colliding outflow boundaries between the merger cell and supercell tilted environmental horizontal vorticity into the vertical such that a new midlevel mesocyclone developed. This mesocyclone eventually merged with the main El Reno mesocyclone and was marked by rapid intensification and the production of an EF5 tornado shortly thereafter.

While previous literature acknowledges that cell mergers often do play a role in supercell behavior, anticipating whether the merger will be constructive or destructive with respect to mesocyclone strength is challenging. A climatological assessment of the frequency of cell merging events with right-moving discrete supercells and how often these cell mergers are constructive versus destructive to storm rotation does not exist. Such a study may be helpful to forecasters as a guidance tool for predicting the likelihood of a mesocyclone strengthening in right-moving discrete supercells soon after a cell merger. While there are previous studies that attempt to quantify the overall influences of cell merger events on tornadic storms (e.g., Lee et al. 2006; Rogers and Weiss 2008; Rogers 2012), *quantification of cell merger frequency in association with rotational trend data of a substantial number of right-moving discrete supercells like the one presented here has yet to be completed*.

This study presents an examination of 342 supercells from 2003 to 2011. Each storm was manually analyzed to identify cell merging time(s), and azimuthal shear data were extracted for each storm so that constructive or destructive cell merger behaviors could be analyzed. We acknowledge that there are many other local environmental inhomogeneities that can lurk in the inflow of supercells (horizontal convective rolls, gravity waves, outflow boundaries, etc.) and more gradual inhomogeneities may also exist simply due to synoptic-scale thermodynamic and kinematic gradients in the warm sector, and that all of these may play a role in azimuthal shear evolution. In this paper, we focus on cell mergers and their association with mesocyclone evolution for conciseness.

Brought to you by NOAA Central Library | Unauthenticated | Downloaded 03/14/22 08:34 PM UTC

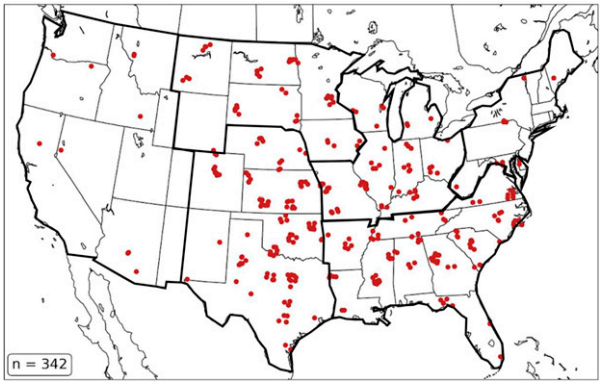

FIG. 1. Map of the 342 severe weather reports associated with the supercells analyzed in this study. All reports occurred within 20–40 km of a NEXRAD WSR-88D instrument between 2003 and 2011 and were associated with discrete, right-moving supercells. The six regions used in this study (West, Northern Plains, Great Plains, Midwest, South, and Northeast) are outlined. As in Anderson-Frey et al. (2018), Montana is split at 110°W, Wyoming is split at 109°W, and Colorado and New Mexico are split at 107°W.

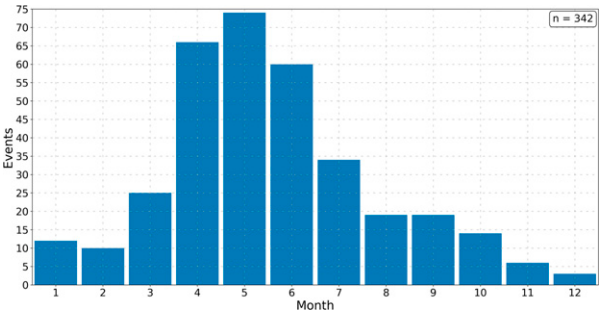

FIG. 2. Histogram of the number of supercells (n = 342) falling within each month of the year.

2. Data and methods

a. Building the supercell dataset

This study features a manually compiled dataset of tornado and significant[1] severe (hereinafter referred to simply as "severe") weather reports that occurred between 2003 and 2011 in the contiguous United States. The dataset is drawn from the more comprehensive database presented in Smith et al. (2012) containing 22901 reports during the same time frame but associated with all storm modes (discrete, clusters, quasi-linear convective systems, etc.). In this study, we limit our analysis to reports associated with thunderstorms that were classified as discrete, right-moving supercells at the time that they produced a report within 20–40 km of a NEXRAD WSR-88D site. We analyzed events from 2003 to 2011 for two reasons: 1) to build a sample size large enough to test for statistical significance that was feasible to accomplish in a reasonable amount of time, and 2) to ensure consistency in the supercells that were analyzed. Only tornado and *significant* wind/hail reports are included from 2003 to 2012 in the Smith et al. (2012) database (i.e., nontornadic supercells that only produced nonsignificant wind/hail reports were not included). The dataset used to analyze mesocyclone evolution (described in section 2c) is currently available from 1998 to 2011. In this study, we analyze all events in the overlapping years between the two datasets (2003–11). We focus only on discrete, right-moving supercells because we hypothesize that the manner in which azimuthal shear evolution is influenced by cell mergers may change based on the storm mode. We focus on storms within 20–40 km of a radar site for two reasons: 1) this yielded a final sample size that was large enough to make generalizable conclusions but small enough for our group to analyze in a reasonable amount of time, and 2) to ensure sufficient and consistent radar coverage at low levels [e.g., within the lowest 1 km above ground level (AGL)] for the azimuthal shear and cell merger analyses during the time frame over which the analyzed storms exhibited supercellular characteristics. After applying these constraints on storm mode and distance from the nearest radar site, our dataset included 561 severe weather reports.

Next, radar data for each case were downloaded and analyzed using GR2-Analyst, an application useful for displaying Level-II NEXRAD data. Report locations were synthesized with radar data to manually match each report with its parent supercell. This yielded 470 individual supercells (some produced more than one report). Some candidate supercells (128) were not included for a variety of reasons, including the following:

- insufficient radar data were available during the event,
- tornado report appeared to be a land spout rather than a mesocyclonic tornado,
- tornado or wind report occurred in a tropical cyclone rainband, and
- report uncertainty (e.g., timing and/or location) made it impossible to locate the parent storm.

Removing these storms yielded a final dataset of 342 supercells. Figures 1 and 2 show the location and month of the report associated with each supercell. The spatial and diurnal maxima in severe weather occurrence are consistent with the climatologies presented in Brooks et al. (2003, their Figs. 3–6) and Smith et al. (2012, their Figs. 6–7 and 11). The paths of these supercells were then analyzed along the segment in which they were within 75 km of the nearest radar site. Consistent with our methods thus far, this subjective threshold was chosen to ensure sufficient radar coverage at low levels; 75 km is the distance at which a 0.5° sweep (the typical WSR-88D lowest-tilt radar scan) reaches a height near 1 km above radar level. The track analysis included noting the times of any cell mergers and extracting azimuthal shear time series, described next.

[1] A significant severe event is defined as an F/EF2+ tornado, a wind gust of 65 kt (33.4 m s^{-1}) or greater, or hail of 2 in. (5.1 cm) or greater.

Brought to you by NOAA Central Library | Unauthenticated | Downloaded 03/14/22 08:34 PM UTC

b. Identifying cell mergers along supercell tracks

Cell mergers were identified along each supercell's track by examining Level-II radar reflectivity data. Identifying cell mergers is not an easily automated process and required a large amount of attention to detail; to the best of our ability, we noted a cell-merger time when the core of a discrete cell (typically containing lowest-elevation-scan reflectivity of 35+ dBZ) merged with the core (typically the 35+-dBZ outline) of the primary supercell. We often used the lowest available elevation scan to do this. Merger times were not interpolated between radar scan times (i.e., the smallest possible time between successive cell mergers was the time of a single radar volume update: 5–6 min). This introduced some complications because reflectivity characteristics of the primary supercell and merging cells can change substantially between successive volume scans; however, we found that circumstances like this were rare (1–2 storms) and would not qualitatively impact our findings. This complication could be addressed in future studies by analyzing storms sampled by radars with greater temporal resolution.

Each coauthor contributed to manual cell-merger identification and completed at least one year of analyses (some completed two). To help ensure consistency, we initially examined a subset of 10 supercells. We then compared our results, discussed any differences, and finalized our approach before completing our respective analyses. It is also worth noting that we considered characterizing other aspects of cell mergers (such as the maximum reflectivity of the merging cell, supercell-relative location of the merger, etc.) but deduced that consistency across our analyses (i.e., between the coauthors; intercoder reliability) for these variables would be too low for meaningful quantitative analysis. The time resolution of the radar data (updates every 5 min) was also a limiting factor here, as the location of the merging cell with respect to the primary supercell may change by impactful distances (e.g., several kilometers; Hastings and Richardson 2016) during this time window and introduce large error. We discuss the known influences of some of these characteristics on mesocyclone strength in section 5.

c. Extracting azimuthal shear time series

We used the Multi-Year Reanalysis of Remotely Sensed Storms (MYRORSS; Williams et al. 2021) database to quantify supercell evolution in terms of low-level mesocyclone strength. This database merges radar data from all NEXRAD WSR-88D sites in the contiguous United States to create gridded fields of radar-derived products (Lakshmanan et al. 2006).[2] These products include the maximum expected size of hail and severe hail index (Witt et al. 1998), echo tops (Lakshmanan et al. 2013), vertically integrated liquid (Greene and Clark 1972), and azimuthal shear (Mahalik et al. 2019). We focus on the azimuthal shear product in this study (particularly at low levels), which uses a linear, least squares derivative approach to quantify the gradient of the scalar azimuthal and radial components that is fit to its local neighborhood (e.g., Smith and Elmore 2004; Miller et al. 2013; Mahalik et al. 2019). The result is a merged azimuthal shear from 0 to 3 km AGL on a horizontal grid with a resolution of 0.005° latitude and longitude (around 500 m on average). The data are available roughly every 5 min.

The 342 supercells were analyzed for the duration of their lifespan that they resided within 75 km of the nearest radar site. For many storms, this yielded an azimuthal shear time series for their entire life cycles; for others, this yielded an azimuthal shear time series for a portion of their life cycles. For supercells that initiated within 75 km of the nearest radar site, we started tracking azimuthal shear around the time when an identifiable low-level mesocyclone (near 1 km AGL) appeared on the radial velocity presentation. For supercells that decayed within 75 km of the nearest radar site, we stopped tracking azimuthal shear around the time when the identifiable low-level mesocyclone (near 1 km AGL) dissipated on the radial velocity presentation. For supercells that moved into or out of the area within 75 km of the nearest radar site, we began or stopped tracking azimuthal shear at the time that it moved into or out of that region, respectively. To reiterate, all of these 342 supercells produced at least one severe weather report within 20–40 km of the nearest radar site and were tracked for the entire time that they remained within 75 km of that radar site.

We "tracked" each supercell by defining a start/end time, latitude, and longitude for the desired period of analysis. These times and coordinates were used to define a constant motion vector. For cases where the supercell deviated from a constant motion, the analysis was broken into segments to more closely follow the actual storm track. A 10-km-wide search box was then moved through the domain at a speed and bearing equal to the motion vector. Of course, actual supercell motions were never exactly constant during their analysis periods; in our cases, the 10-km-wide search box was wide enough to allow for deviations from the constant box motion while remaining focused on the storm of interest. At each time step (roughly every 5 min), we objectively noted the location and value of the low-level (0–3 km AGL) azimuthal shear maximum within the search box. The result was a time series of maximum low-level azimuthal shear and its track during the entire analysis period. In this study, we use this time series to represent mesocyclone evolution in the lowest 3 km AGL. This best represents what is commonly referred to as the "low level" mesocyclone but may also be influenced by characteristics of the lower part of the "midlevel" mesocyclone (e.g., 2–3 km AGL). Acknowledging this, we refer to the mesocyclone in the 0–3-km layer as the low-level mesocyclone for the remainder of the paper. Figure 3 shows a histogram of the number of azimuthal shear analysis times (binned each hour) during the convective day; the peak occurs around 2200 UTC, which is consistent with the subdaily severe thunderstorms found in Krocak and Brooks (2020, see their Figs. 5 and 6). On the basis of the consistencies of our spatial, monthly, and subdaily climatologies with prior work containing larger datasets, we believe that our findings about the

[2] Quality control methods for this database are described in Lakshmanan et al. (2007, 2010).

Brought to you by NOAA Central Library | Unauthenticated | Downloaded 03/14/22 08:34 PM UTC

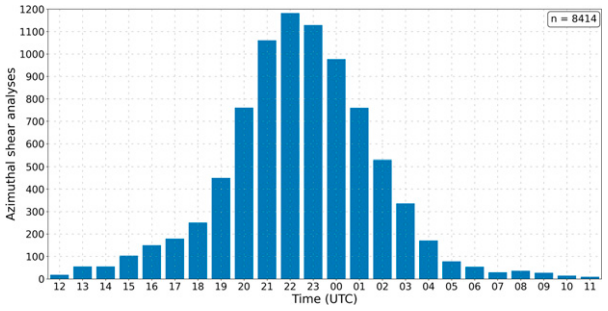

FIG. 3. Histogram of the number of azimuthal shear analysis times (n = 8414) across all supercells (n = 342) that fall within each hour of the convective day (demarcated at 1200 UTC).

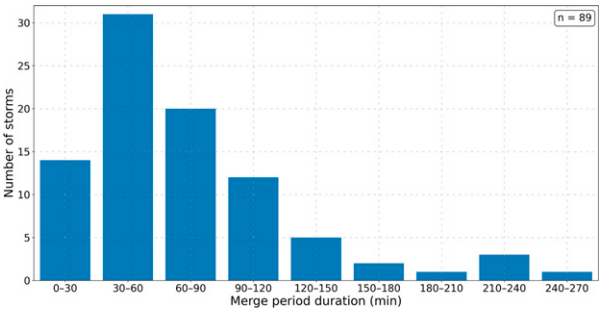

FIG. 5. Histogram of the number of supercells with more than one merger (n = 89) binned by the time between the initial and final cell merger (every 30 min).

climatology of cell mergers and their association with supercell evolution are generalizable. These results are presented in the next two sections.

3. Merger climatology

In our dataset of 342 supercells, 166 (49%) experienced at least one merger during their analysis periods. Of those 166 supercells, 89 (53%) experienced more than one. Based on Fig. 4, most of the supercells that experienced mergers encountered 1–5. The maximum number of mergers that any individual cell encountered was 13. The mean and median numbers of mergers per storm were 2.31 and 2, respectively. The maximum number of mergers per hour was near 5.67, or roughly once every 10.5 min, and the median was near 0.93, roughly once per hour.

For the subset of supercells that experienced more than one merger (n = 89), Fig. 5 shows the distribution of the time difference between the first and last merger that each storm experienced. Of these supercells, most of them experienced mergers within a 90-min period during the time they were analyzed. However, this finding is probably sensitive to the fact that we did not systematically document the *entirety* of every supercell's life cycle. Therefore, this represents the lower bound of the amount of time during a supercell's life cycle that it may experience multiple cell mergers. For the same subset of supercells, Fig. 6 shows a histogram of the time differences between successive mergers for each storm; n = 217 represents the total number of mergers across these 89 supercells. Recall that the time differences are limited to intervals of 5 min. Around one-half (45%) of the 217 individual cell mergers included here occurred within 30 min of each other. This arbitrary threshold (30 min between successive cell mergers) is used later to define cell merger "events" (e.g., mergers that occurred within 30 min of each other are denoted as a single cell merger event). In section 4, we use this definition to examine azimuthal shear evolution before, during, and after cell merger events.

Counts of cell merger occurrence (and the lack thereof) in each region of the United States are shown next in Fig. 7 (i.e., the sum of the blue and red bars) in each region is similar to the climatological frequencies of regional supercell occurrence, using regions defined as in Anderson-Frey et al. (2018) (see Fig. 1). Of more interest to us is the fraction of supercells in each region that experience cell mergers. We hypothesized that differences—if there were any—in this fraction between different regions would be due to differences in the typical environments of supercells in each region (e.g., Sherburn and Parker 2014). Among regions with more than 30 cases, the South (55.6%) and the Great Plains (52.5%) exhibit the highest fraction of cases featuring one or more mergers during the analysis period, while the Northern Plains (43.5%) and Midwest (37.9%) cases feature slightly fewer mergers. The Northeast experiences the smallest fraction of mergers overall

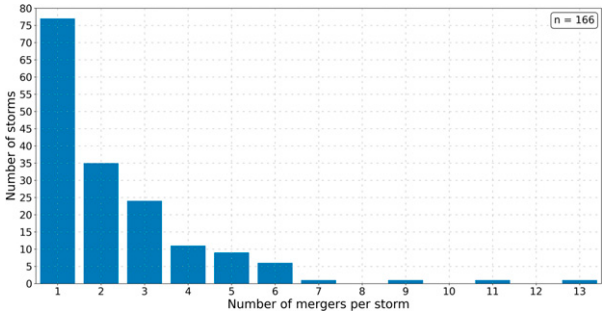

FIG. 4. Histogram of the number of supercells that experienced a certain number of cell mergers during their analysis period (indicated on the x axis).

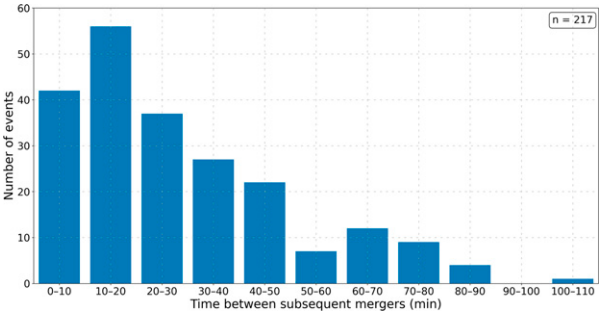

FIG. 6. Histogram of the number of mergers (n = 217) that occurred in the 89 supercells experiencing more than one merger, binned by the time between successive mergers (every 10 min).

Brought to you by NOAA Central Library | Unauthenticated | Downloaded 03/14/22 08:34 PM UTC

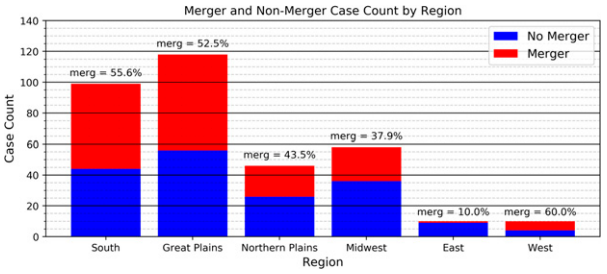

FIG. 7. Counts of supercells in each region of the contiguous United States demarcated by whether each one experienced a cell merger (red) or did not (blue). The total case count in each region is given by the *y* axis, and the percentage of all supercells that experienced a merger within each region is indicated at the top of each bar.

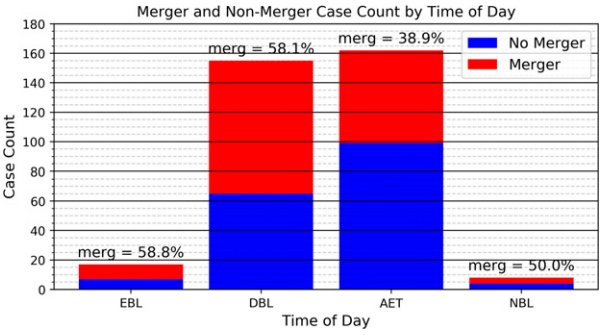

FIG. 9. As in Fig. 7, but for counts of supercells grouped by the time of day in which they occurred. The definitions of each time-of-day bin, which were drawn from Lyza and Knupp (2018), are found in the text.

(10.0%), while the West features the greatest fraction (60.0%). However, these last two findings may not be robust because of the small sample sizes in each region (n = 10 supercells for both).

Figure 8 is similar to Fig. 7 except it shows counts of cell merger occurrence based on the meteorological season. Slight differences in merger frequency are noted across seasons, with mergers slightly more frequently observed in meteorological autumn (September–November; 56.4% of cases) and winter (December–February; 52.0%) than spring (March–May; 46.1%) or summer (June–August; 49.6%). We show the same cell merger count except discretized by time of day in Fig. 9. We split the diurnal cycle into four 6-h periods in line with the methods of Lyza and Knupp (2018) to roughly approximate four periods within a typical boundary layer cycle: the early boundary layer (EBL), describing the morning destabilization period of the boundary layer; the diurnal boundary layer (DBL), or period with relatively low boundary layer static stability; the afternoon-evening transition (AET), the transition period after the DBL period; and the nocturnal boundary layer (NBL), featuring relatively high boundary layer static stability. Since the definitions for each time period were defined in the central time zone in Lyza and Knupp (2018), the ranges defining each period were adjusted for the time zone location of the analysis radar. Unsurprisingly, the overwhelming majority of supercells in our dataset occurred during the DBL (155 out of 342 cases) and AET (162 cases), whereas the EBL (17) and NBL (8) comprise sample sizes of an order-of-magnitude fewer. The EBL and DBL feature nearly identical fractions of cases with mergers observed during the analysis period (58.8% and 58.1%, respectively), while the AET (38.9%) and NBL (50.0%) feature fewer cases with mergers. Comparison of the merger frequencies across all four time periods is hampered by the small number of cases in the EBL and NBL time periods. As such, if the 24-h diurnal cycle is instead broken into two periods with different boundary layer characteristics (EBL–DBL and NBL–AET), the combined EBL and DBL observed merger frequency is 58.1% (n = 172 cases) and the combined AET and NBL observed merger frequency is 39.4% (n = 170 cases).

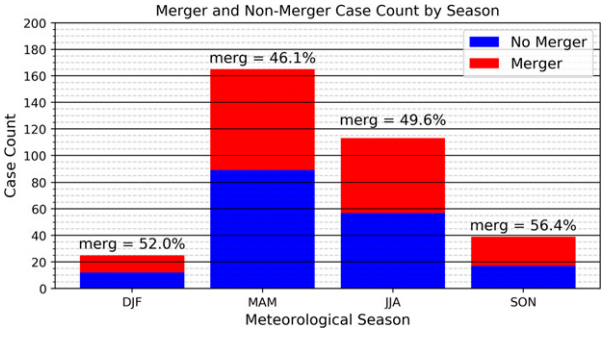

FIG. 8. As in Fig. 7, but for counts of supercells grouped by the meteorological season in which they occurred [December–February (DJF), March–May (MAM), June–August (JJA), and September–November (SON)].

4. Azimuthal shear evolution during cell mergers

We now document our findings on azimuthal shear evolution in association with cell merger events. In the following figures and discussion, we define a cell merger "event" as the time period(s) for each storm in which it experienced one or more cell mergers within a 30-min period. All of these individual cell mergers were then combined and considered a single event for the purposes of analyzing azimuthal shear evolution. For example, if four cell mergers occurred every 20 min in succession, all four of those individual mergers would be considered a single event. If a fifth merger occurred 40 min after the last of those four, it would be considered a separate cell merger event. This process was conducted for each supercell experiencing at least one cell merger. Using this definition, the number of cell merger events experienced by any supercell ranged from 1 to 3. It is straightforward to change the time period of a cell merger event in this framework (e.g., from 30 to 15 min). In general, our results are insensitive to changes in the time period.

We used this approach to analyze relationships between azimuthal shear evolution and cell merger *events* (rather than individual cell merger occurrence) to be able to calculate averaged azimuthal shear quantities before and after each event. Many storms experienced several cell mergers, often close in

Brought to you by NOAA Central Library | Unauthenticated | Downloaded 03/14/22 08:34 PM UTC

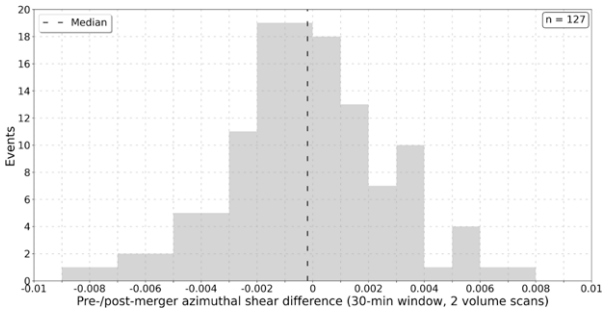

FIG. 10. Histogram of the difference between post- and premerger azimuthal shear for the 127 supercells that experienced at least one merger event and contained sufficient MYRORSS data for this analysis. As described in the text, a merger "event" is defined as the collection of all mergers that occur within successive 30-min periods. The azimuthal shear difference is found by subtracting the mean postmerger value from the mean premerger value. Mean azimuthal shear values are found using the two volume scans either immediately before or after the merger event. The differences are binned every 0.001 s^{-1}. The dashed, black vertical line represents the median of the distribution.

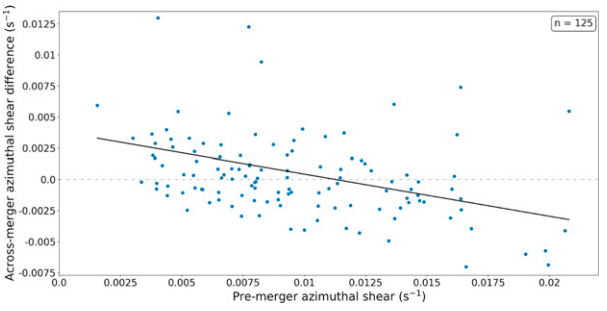

FIG. 11. Scatterplot of 125 supercells that experienced at least one merger event and contained sufficient MYRORSS data to analyze premerger azimuthal shear (x axis) and the difference between post- and premerger azimuthal shear (y axis). As in Fig. 10, a merger "event" was defined as the collection of any mergers that occurred within successive 30-min periods, and mean pre-/postmerger azimuthal shear values were calculated using the two volume scans either immediately before or after the merger event. The statistically significant best fit line is shown. Two outliers with premerger azimuthal shear > 0.03 s^{-1} are omitted from this analysis.

time to each other. As a result, using a temporal average of azimuthal shear, over perhaps 10–15 min, incorporated the same azimuthal shear value for multiple instances of pre- or postmerger mean azimuthal shear. This introduces problems in the degrees of freedom for statistical calculations because different groups of pre- or postmerger mean azimuthal shear may be influenced by the same individual azimuthal shear value(s). Furthermore, we believe that the dynamical response of a supercell to multiple cell mergers in succession may be different than its dynamical response to a single cell merger. As will be discussed later, this appears to be true.

The first question we ask about the association of cell merger events with azimuthal shear evolution is, Does azimuthal shear typically increase, decrease, or stay the same before and after a cell merger event? Figure 10 shows a histogram of the difference in azimuthal shear before and after cell merger events. The pre- and postmerger azimuthal shear values used to calculate the difference are the mean azimuthal shear values in the two volume scans before and after the event. Of the 166 supercells that experienced mergers, 127 of them contained sufficient data to calculate both pre- and postmerger azimuthal shear values. (In other words, the time of the first merger occurred 30 min after the azimuthal shear time series began, or vice versa with respect to the last merger.) The median difference is small, around -0.0002 s^{-1}. Most cases are centered around zero within the range from -0.003 to 0.003 s^{-1}. There appear to be a few more cases that undergo significant decreases in azimuthal shear (e.g., < -0.005 s^{-1} decrease) rather than those that undergo significant increases. In any case, we believe that this result confirms our current understanding of the widely varying influence of cell mergers on supercell morphology; any relationships between cell mergers and resulting mesocyclone evolution are likely linked to storm-scale characteristics of the primary supercell, merging cell, and perhaps even the local environment, only some of which are represented here. In addition, the effects of other factors that influence mesocyclone evolution—such as the rate of supercell development in different background environments, environmental inhomogeneities external to the cell merger, and so on—add complexity to any broad relationships between cell mergers and mesocyclone strength.

Next, we address whether differences in azimuthal shear before and after cell merger events are related to premerger azimuthal shear. In other words, are weaker mesocyclones more likely to decay after a cell merger than stronger mesocyclones? Figure 11 shows a scatterplot of the difference in azimuthal shear before and after cell merger events as a function of premerger azimuthal shear. Two outlier events that contained premerger azimuthal shear >0.03 s^{-1} are omitted from this analysis,[3] yielding a final sample size of 125 supercells that experienced at least one merger event. The results are somewhat surprising to us; stronger mesocyclones appear more susceptible to the detrimental effects of cell merger events than weaker mesocyclones. The linear best fit is shown, which has $R^2 = 0.12$ and $p = 5.7 \times 10^{-5}$ from a Student's t test.[4] The RMSE for this fit is approximately 0.0043 s^{-1} (around 15% of the range of across-merger azimuthal shear

[3] These two events were classified as "outliers" because their premerger mean azimuthal shear values exceeded the standard upper limit of a box-and-whisker distribution of the data. The upper limit is defined as Q3 + 1.5 × IQR, where Q3 is the 75th percentile of the data and IQR is the interquartile range (Q3 − Q1, where Q1 is the 25th percentile). This yielded an upper limit of 0.022 s^{-1}.

[4] Multiple across-merger azimuthal shear differences from the same storm were included in this test because of the small decorrelation time scale of the azimuthal shear time series. In particular, we analyzed the decorrelation time scales of a mean azimuthal shear time series calculated by taking the mean of corresponding, adjacent pairs of the original azimuthal shear values. This yielded mean decorrelation time scales that were approximately two volume scans (10 min).

Brought to you by NOAA Central Library | Unauthenticated | Downloaded 03/14/22 08:34 PM UTC

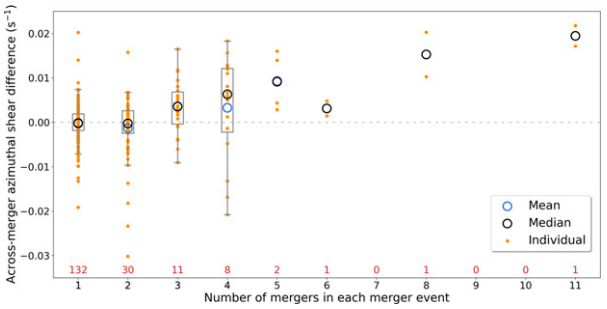

FIG. 12. Scatterplot of the difference between post- and pre-merger azimuthal shear—for the 127 supercells that experienced at least one merger and contained sufficient MYRORSS data for this analysis—binned by the number of individual mergers within each merger event. Merger events and across-merger azimuthal shear differences were analyzed in the same time windows as in Figs. 10 and 11. The number of merger events in each bin is indicated by the red text near the bottom of the plot. The mean (blue) and median (black) of each distribution are shown with an open circle. The entire distribution in each bin is also shown (orange) along with a box-and-whisker plot for the larger sample sizes. The box shows the interquartile range (IQR) with the whiskers extending 1.5 × IQR in either direction (or to the last data point if it lies within this range).

difference values). Although this R^2 value is very small, we believe this relationship is physically significant given the range of values shown in Fig. 11 and relatively small RMSE.

We next examine whether differences in azimuthal shear before and after cell merger events are related to the number of individual mergers in each event. In other words, are mesocyclones more likely to weaken after longer periods of successive individual mergers, or vice versa? Figure 12 shows a scatterplot of the difference in azimuthal shear before and after cell merger events as a function of the number of individual cell mergers within each cell merger event. To reiterate, this plot employs the same definition of a cell merger event as above in which mergers that occurred within 30 min of each other are considered the same "merger event." Using this definition, the largest number of individual mergers within a single merger event was 11. The overwhelming majority of merger events contained 1–4 individual mergers (indicated by the red text near the bottom of each distribution). The means and medians of the azimuthal shear difference for each number of individual cell mergers are shown and reveal a generally positive trend. Azimuthal shear differences are not very different between merger events with 1 or 2 individual mergers, but as the number of individual mergers increases to 3 and 4, the azimuthal shear difference tends to increase. In other words, as the time duration and number of individual cell mergers within the merger event increase, azimuthal shear is more likely to increase. The same general trend continues for merger events with more individual mergers, but the sample size (indicated by the red text along the x axis) is too small to extend our physical claim to that part of the distribution.

5. Discussion

The climatological analysis of merger frequency reveals primarily subtle seasonal, temporal, and spatial variations in observed merger frequency. As discussed in section 3, mergers are slightly more frequently observed in meteorological autumn and winter than spring or summer. While it may be hypothesized that seasonal differences in elevated mixed layer strength and resulting convective inhibition (CIN) values might result in differences in convective coverage and merger frequency, the smaller sample sizes of autumn and winter cases (<50% of the spring and summer sample sizes) and the lack of assessment of overall convective coverage for each case prohibit confidently identifying any cause for these differences. Likewise, there are more cases with observed mergers in the South and the Great Plains than in the Northern Plains and Midwest, but the physical reasons for these differences remain rather unclear.

The greatest climatological differences in merger frequency, those observed between the EBL/DBL and AET/NBL time periods, may be somewhat physical. We hypothesize that the higher incidence of observed mergers during the EBL and DBL periods may be linked to lower boundary layer static stability and lower CIN magnitudes (e.g., closer to 0 J kg^{-1}) relative to the AET and NBL periods. Lower CIN magnitudes, in turn, could lead to greater convective coverage and a higher probability or incidence of cell mergers. Further study of the environments of supercells that do and do not exhibit cell mergers is beyond the scope of this study and would be useful in investigating what processes are relevant in governing relationships between supercell evolution and cell merger occurrence.

The result that azimuthal shear does not change significantly across all merger events is not very surprising. Both observational and modeling supercell studies have shown that in some cases, cell mergers yield a strengthening mesocyclone (or even tornadogenesis), and in others yield a weakening one. In the modeling study of Hastings and Richardson (2016), this outcome was sensitive to the strength of the merging cell's cold pool and the distance between the primary updrafts of the supercell and merging cell. The tornado outbreak in central Oklahoma on 24 May 2011 provides a prolific example of this range of outcomes (NWS 2011); two violently tornadic supercells weakened rapidly after merging with a left-moving supercell, while a third right-moving supercell merged with a weaker storm, rapidly strengthened, and produced an EF5 tornado (Tanamachi et al. 2015). Our finding that low-level azimuthal shear does not generally increase or decrease following cell merger events corroborates these studies. Another reason that we did not find a general relationship between cell mergers and azimuthal shear evolution is probably because a number of other factors influence mesocyclone strength, such as characteristics of the background environment, spatiotemporal inhomogeneities in addition to cell mergers, and so on. More significant trends may be discovered by thresholding on additional storm or environmental characteristics, like the strength of the merging cell [cold pool strength, overshooting top height, or (anti)cyclonic mesocyclone

Brought to you by NOAA Central Library | Unauthenticated | Downloaded 03/14/22 08:34 PM UTC

strength], boundary layer humidity in the environment, and so on.

Thresholding the outcome of merger events on characteristics of the supercell or merger event yielded (sometimes significant) relationships. Particularly, a stronger low-level mesocyclone is more likely to be negatively impacted by cell mergers. Furthermore, merger events with 1–2 individual mergers are more likely to impede or reverse mesocyclone intensification than merger events with 3–4 individual mergers. In other words, shorter merger events are more likely to yield a steady or weakening low-level mesocyclone; longer merger events are more likely to yield a strengthening low-level mesocyclone. Both of these findings seem somewhat counterintuitive. Part of these relationships, especially with respect to premerger azimuthal shear and subsequent azimuthal shear evolution, may be artificially influenced by our methods. Particularly, if a merger event yielded a rapidly weakening low-level mesocyclone, it may have not been tracked for long enough after the merger to contain sufficient azimuthal shear data for further analysis. This would bias supercells with weak premerger low-level mesocyclones toward strengthening after merger events and vice versa for supercells with strong premerger low-level mesocyclones. However, these findings also may give clues as to what physical processes are most important in influencing supercell morphology at different stages of its life cycle. Perhaps in the early developmental stages—when the establishment of the low- and midlevel mesocyclone occurs via tilting of ambient horizontal vorticity (e.g., Davies-Jones 1984)—any process by which a storm-scale updraft is forced may have a beneficial effect. Once a strong mesocyclone is established, it then might generally favor a steady background environment that is then locally enhanced by the storm itself (e.g., Nowotarski and Markowski 2016; Wade et al. 2018; Flournoy et al. 2020); perhaps any disruptions at this point, however brief, are more likely to yield mesocyclone weakening. These ideas are speculative but hopefully motivate future work on how storm- and larger-scale processes influencing supercell morphology may change based on the varying supercell and environmental characteristics at different times.

We believe that the climatological aspects of this study are generalizable to right-moving supercells in the contiguous United States (except perhaps in the West and Northeast regions where sample sizes are much smaller). The locations and times of the supercell tracks analyzed here are consistent with published supercell and tornado climatologies (Brooks et al. 2003; Smith et al. 2012; Krocak and Brooks 2020). Furthermore, this study features a very large database of supercells (n = 342) that documents storm-scale evolution in association with environmental characteristics (in this case, cell mergers). However, for reasons previously discussed, we limited our focus to the portions of all supercell tracks within 75 km of the nearest WSR-88D site. This means that the raw numbers of individual mergers and merger events per supercell, as well as the fraction of all supercells that experience cell mergers, are lower-bound values; because not every supercell prefers to visit the closest WSR-88D site, the actual numbers are almost certainly higher. However, we believe our sampling methodology and analysis framework is sufficient to yield informative statistics on merger characteristics (or lack thereof) within the portions of the supercells that were observed.

6. Summary and conclusions

In this study, we compiled radar and azimuthal shear data for 342 right-moving supercells to 1) build a climatology of cell mergers and 2) examine how azimuthal shear associated with the mesocyclone is influenced by cell mergers. These events were drawn from a much larger database of tornado and significant severe weather reports in the contiguous United States from 2003 to 2011. The events were selected because of their close proximity to WSR-88D sites, which we used to analyze each supercell's morphology and association with cell mergers.

Our most important findings related to the cell merger climatology are as follows:

- *Many supercells experience cell mergers*. Almost one-half (49%) experienced at least one cell merger in the analysis period. Over a quarter (26%) experienced more than one. These values represent the lower-bound frequency for merger occurrence because in many cases we only focused on a portion of many of the supercells' life cycles. As merging cells lead to a significant spatiotemporal heterogeneity, this calls into question how well simulated supercell evolution in homogeneous environments broadly represents observed supercell evolution in more complex environments.
- *The frequency of cell mergers varies somewhat by region.* Supercells in the South and Great Plains regions experience cell mergers over 50% of the time, whereas those in the Northern Plains and Midwest experience them around 40% of the time. We cannot confidently assess the frequency of cell mergers in the Northeast or West regions because of smaller sample sizes relative to the other four regions.
- *The frequency of cell mergers varies somewhat by time of day.* Supercells occurring within the diurnal boundary layer-period experience mergers almost 60% of the time, while those occurring within the afternoon–evening transition-period experience mergers around 40% of the time.

Our most important findings related to the association of cell merger events with low-level mesocyclone evolution are as follows:

- *No generally applicable temporal relationship exists between cell merger events and the evolution of low-level azimuthal shear*. This corroborates previous studies and numerous anecdotal accounts suggesting that the outcome of a merger event, with respect to low-level mesocyclone strength, is highly sensitive to characteristics of the supercell, merging cell, and environment that were not accounted for in this study (merging cell strength, boundary layer humidity, other environmental inhomogeneities, etc.).
- *Stronger low-level mesocyclones are more likely to weaken during cell merger events, and vice versa for weaker low-level mesocyclones*. Although this might be somewhat

Brought to you by NOAA Central Library | Unauthenticated | Downloaded 03/14/22 08:34 PM UTC

counterintuitive, it highlights that the way in which storm-scale processes influence low-level mesocyclone strength may change depending on supercell maturity.

- *Cell merger-influenced mesocyclone evolution may be sensitive to the duration of the cell merger event.* As the number of individual cell mergers within a larger merger event increases from 1–2 to 3–4, it is more likely that the low-level mesocyclone strengthens.

This study featured an initial analysis of cell merger occurrence along supercell tracks and their relationship with low-level mesocyclone evolution. Several questions arose that could be addressed either with this dataset or an expanded one. What environmental characteristics influence the resulting low-level mesocyclone strength after a cell merger? Why are stronger low-level mesocyclones more susceptible to weakening during a cell merger event? Why is a longer merger event duration more likely to yield a strengthening low-level mesocyclone? What are the physical processes governing these relationships? Are these trends present in most supercell environments, or are they more sensitive? Thresholding merger outcomes on environmental conditions (boundary layer relative humidity, bulk shear, etc.) is an important next step, but additional supercells would need to be added to this dataset to obtain sufficient sample sizes in each environment. We also believe that further study of supercell morphology at various evolutionary stages is warranted and can be most efficiently achieved with comprehensive observational studies like this one, targeted modeling studies, and higher-resolution analysis of events occurring during field campaigns. This will help interested members of the community in anticipating low-level mesocyclone evolution in real time due to environmental inhomogeneities like cell mergers.

Acknowledgments. We are grateful for many insightful conversations with Erik Rasmussen that solidified the ideas for this project. We are also grateful to him for reviewing an early draft of the paper. We thank the forecasters at the Storm Prediction Center, particularly Rich Thompson, John Hart, and Bryan Smith, for their guidance in the beginning stages of this project. We also thank Anthony Reinhart for his help in accessing and working with the MYRORSS dataset. We are grateful for the efforts of Skylar Williams, Kiel Ortega, Travis Smith, and others in creating it. We also thank three anonymous reviewers who improved this study. Funding was provided by NOAA/Office of Oceanic and Atmospheric Research under NOAA–University of Oklahoma Cooperative Agreements NA16OAR4320015 and NA21OAR4320204, U.S. Department of Commerce. Author M. Flournoy was funded on a postdoctoral fellowship through the Cooperative Institute for Severe and High-Impact Weather Research and Operations. Author A. Lyza was funded through the NOAA VORTEX-SE Program. Authors M. Satrio and M. Diedrichsen were funded by the National Science Foundation Grant AGS-1824811. The statements, findings, conclusions, and recommendations are those of the authors and do not necessarily reflect the views of NOAA or the U.S. Department of Commerce.

Data availability statement. The radar data analyzed in this study are available on the NEXRAD NCEI online database (https://www.ncdc.noaa.gov/nexradinv/). The MYRORSS data are also available online (https://osf.io/9gzp2/). The Smith et al. (2012) storm-report database is available upon request to the first author.

REFERENCES

Anderson-Frey, A. K., Y. P. Richardson, A. R. Dean, R. L. Thompson, and B. T. Smith, 2018: Near-storm environments of outbreak and isolated tornadoes. *Wea. Forecasting*, **33**, 1397–1412, https://doi.org/10.1175/WAF-D-18-0057.1.

Bluestein, H. B., and M. L. Weisman, 2000: The interaction of numerically simulated supercells initiated along lines. *Mon. Wea. Rev.*, **128**, 3128–3149, https://doi.org/10.1175/1520-0493(2000)128<3128:TIONSS>2.0.CO;2.

Brooks, H. E., C. A. Doswell, and M. P. Kay, 2003: Climatological estimates of local daily tornado probability for the United States. *Wea. Forecasting*, **18**, 626–640, https://doi.org/10.1175/1520-0434(2003)018<0626:CEOLDT>2.0.CO;2.

Bryan, G. H., J. C. Wyngaard, and J. M. Fritsch, 2003: Resolution requirements for the simulation of deep moist convection. *Mon. Wea. Rev.*, **131**, 2394–2416, https://doi.org/10.1175/1520-0493(2003)131<2394:RRFTSO>2.0.CO;2.

Davies-Jones, R. P., 1984: Streamwise vorticity: The origin of updraft rotation in supercell storms. *J. Atmos. Sci.*, **41**, 2991–3006, https://doi.org/10.1175/1520-0469(1984)041<2991:SVTOOU>2.0.CO;2.

——, 2002: Linear and nonlinear propagation of supercell storms. *J. Atmos. Sci.*, **59**, 3178–3205, https://doi.org/10.1175/1520-0469(2003)059<3178:LANPOS>2.0.CO;2.

Flournoy, M. D., M. C. Coniglio, E. N. Rasmussen, J. C. Furtado, and B. E. Coffer, 2020: Modes of storm-scale variability and tornado potential in VORTEX2 near- and far-field tornadic environments. *Mon. Wea. Rev.*, **148**, 4185–4207, https://doi.org/10.1175/MWR-D-20-0147.1.

Greene, D. R., and R. A. Clark, 1972: Vertically integrated liquid water—A new analysis tool. *Mon. Wea. Rev.*, **100**, 548–552, https://doi.org/10.1175/1520-0493(1972)100<0548:VILWNA>2.3.CO;2.

Hastings, R., and Y. Richardson, 2016: Long-term morphological changes in simulated supercells following mergers with nascent supercells in directionally varying shear. *Mon. Wea. Rev.*, **144**, 471–499, https://doi.org/10.1175/MWR-D-15-0193.1.

——, ——, and P. M. Markowski, 2014: Simulation of near-surface mesocyclogenesis during mergers between mature and nascent supercells. *27th Conf. on Severe Local Storms*, Madison, WI, Amer. Meteor. Soc., 3B.2, https://ams.confex.com/ams/27SLS/webprogram/Paper255837.html.

Jewett, B. F., R. W. Przybylinski, and R. B. Wilhelmson, 2006: Numerical simulation of the 24 April, 2002 storm merger between a left-moving storm and supercell. *23rd Conf. on Severe Local Storms*, St. Louis, MO, Amer. Meteor. Soc., P11.3, https://ams.confex.com/ams/23SLS/techprogram/paper_115478.htm.

Klees, A. M., Y. P. Richardson, P. M. Markowski, C. Weiss, J. M. Wurman, and K. K. Kosiba, 2016: Comparison of the tornadic and nontornadic supercells intercepted by VORTEX2 on 10 June 2010. *Mon. Wea. Rev.*, **144**, 3201–3231, https://doi.org/10.1175/MWR-D-15-0345.1.

Brought to you by NOAA Central Library | Unauthenticated | Downloaded 03/14/22 08:34 PM UTC

Kogan, Y. L., and A. Shapiro, 1996: The simulation of a convective cloud in a 3D model with explicit microphysics. Part II: Dynamical and microphysical aspects of cloud merger. *J. Atmos. Sci.*, **53**, 2525–2545, https://doi.org/10.1175/1520-0469(1996)053<2525:TSOACC>2.0.CO;2.

Krocak, M. J., and H. E. Brooks, 2020: An analysis of subdaily severe thunderstorm probabilities for the United States. *Wea. Forecasting*, **35**, 107–112, https://doi.org/10.1175/WAF-D-19-0145.1.

Lakshmanan, V., T. Smith, K. Hondl, G. J. Stumpf, and A. Witt, 2006: A real-time, three-dimensional, rapidly updating, heterogeneous radar merger technique for reflectivity, velocity, and derived products. *Wea. Forecasting*, **21**, 802–823, https://doi.org/10.1175/WAF942.1.

——, A. Fritz, T. Smith, K. Hondl, and G. Stumpf, 2007: An automated technique to quality control radar reflectivity data. *J. Appl. Meteor. Climatol.*, **46**, 288–305, https://doi.org/10.1175/JAM2460.1.

——, J. Zhang, and K. Howard, 2010: A technique to censor biological echoes in radar reflectivity data. *J. Appl. Meteor. Climatol.*, **49**, 453–462, https://doi.org/10.1175/2009JAMC2255.1.

——, K. Hondl, C. K. Potvin, and D. Preignitz, 2013: An improved method for estimating radar echo-top height. *Wea. Forecasting*, **28**, 481–488, https://doi.org/10.1175/WAF-D-12-00084.1.

Lee, B. D., B. F. Jewett, and R. B. Wilhelmson, 2006: The 19 April 1996 Illinois tornado outbreak. Part II: Cell mergers and associated tornado incidence. *Wea. Forecasting*, **21**, 449–464, https://doi.org/10.1175/WAF943.1.

Lyza, A. W., and K. R. Knupp, 2018: A background investigation of tornado activity across the Southern Cumberland Plateau terrain system of northeastern Alabama. *Mon. Wea. Rev.*, **146**, 4261–4278, https://doi.org/10.1175/MWR-D-18-0300.1.

Mahalik, M. C., B. R. Smith, K. L. Elmore, D. M. Kingfield, K. L. Ortega, and T. M. Smith, 2019: Estimates of gradients in radar moments using a linear least squares derivative technique. *Wea. Forecasting*, **34**, 415–434, https://doi.org/10.1175/WAF-D-18-0095.1.

Miller, M. L., V. Lakshmanan, and T. M. Smith, 2013: An automated method for depicting mesocyclone paths and intensities. *Wea. Forecasting*, **28**, 570–585, https://doi.org/10.1175/WAF-D-12-00065.1.

Nowotarski, C. J., and P. M. Markowski, 2016: Modifications to the near-storm environment induced by simulated supercell thunderstorms. *Mon. Wea. Rev.*, **144**, 273–293, https://doi.org/10.1175/MWR-D-15-0247.1.

NWS, 2011: The May 24, 2011 tornado outbreak in Oklahoma. NOAA/NWS, accessed 29 October 2020, https://www.weather.gov/oun/events-20110524.

Pozo, D., I. Borrajero, J. C. Marín, and G. B. Raga, 2006: A numerical study of cell merger over Cuba—Part II: Sensitivity to environmental conditions. *Ann. Geophys.*, **24**, 2793–2808, https://doi.org/10.5194/angeo-24-2793-2006.

Rogers, J. W., 2012: Significant tornado events associated with cell mergers. *26th Conf. on Severe Local Storms*, Nashville, TN, Amer. Meteor. Soc., 9.4, https://ams.confex.com/ams/26SLS/webprogram/Paper211575.html.

——, and C. C. Weiss, 2008: The association of cell mergers with tornado occurrence. *24th Conf. on Severe Local Storms*, Savannah, GA, Amer. Meteor. Soc., P3.23, https://ams.confex.com/ams/24SLS/techprogram/paper_141784.htm.

Sherburn, K. D., and M. D. Parker, 2014: Climatology and ingredients of significant severe convection in high-shear, low-CAPE environments. *Wea. Forecasting*, **29**, 854–877, https://doi.org/10.1175/WAF-D-13-00041.1.

Simpson, J., N. E. Westcott, R. J. Clerman, and R. A. Pielke, 1980: On cumulus mergers. *Arch. Meteor. Geophys. Bioklimatol.*, **29A**, 1–40, https://doi.org/10.1007/BF02247731.

Smith, B. T., R. L. Thompson, J. S. Grams, C. Broyles, and H. E. Brooks, 2012: Convective modes for significant severe thunderstorms in the contiguous United States. Part I: Storm classification and climatology. *Wea. Forecasting*, **27**, 1114–1135, https://doi.org/10.1175/WAF-D-11-00115.1.

Smith, T. M., and K. L. Elmore, 2004: The use of radial velocity derivatives to diagnose rotation and divergence. *11th Conf. on Aviation, Range, and Aerospace*, Hyannis, MA, Amer. Meteor. Soc., P5.6, https://ams.confex.com/ams/11aram22sls/techprogram/paper_81827.htm.

Tanamachi, R. L., P. L. Heinselman, and L. J. Wicker, 2015: Impacts of a storm merger on the 24 May 2011 El Reno, Oklahoma, tornadic supercell. *Wea. Forecasting*, **30**, 501–524, https://doi.org/10.1175/WAF-D-14-00164.1.

Tao, W.-K., and J. Simpson, 1989: A further study of cumulus interactions with mergers: Three-dimensional simulations with trajectory analyses. *J. Atmos. Sci.*, **46**, 2974–3004, https://doi.org/10.1175/1520-0469(1989)046<2974:AFSOCI>2.0.CO;2.

Wade, A. R., M. C. Coniglio, and C. L. Ziegler, 2018: Comparison of near- and far-feld supercell inflow environments using radiosonde observations. *Mon. Wea. Rev.*, **146**, 2403–2415, https://doi.org/10.1175/MWR-D-17-0276.1.

Westcott, N. E., 1994: Merging of convective clouds: Cloud initiation, bridging, and subsequent growth. *Mon. Wea. Rev.*, **122**, 780–790, https://doi.org/10.1175/1520-0493(1994)122<0780:MOCCCI>2.0.CO;2.

Williams, S. S., K. L. Ortega, and T. M. Smith, 2021: MYRORSS_-Data. Open Science Framework (Center for Open Science, Inc.), accessed 1 December 2021, https://osf.io/9gzp2/.

Witt, A., M. D. Eilts, G. J. Stumpf, J. T. Johnson, E. D. Mitchell, and K. W. Thomas, 1998: An enhanced hail detection algorithm for the WSR-88D. *Wea. Forecasting*, **13**, 286–303, https://doi.org/10.1175/1520-0434(1998)013<0286:AEHDAF>2.0.CO;2.

Wurman, J., Y. Richardson, C. Alexander, S. Weygandt, and P. F. Zhang, 2007: Dual-Doppler and single-Doppler analysis of a tornadic storm undergoing mergers and repeated tornadogenesis. *Mon. Wea. Rev.*, **135**, 736–758, https://doi.org/10.1175/MWR3276.1.

Brought to you by NOAA Central Library | Unauthenticated | Downloaded 03/14/22 08:34 PM UTC